IOP Conference Series: Materials Science and Engineering



PAPER • OPEN ACCESS

# Thermal characterization of a three-fluid cryogenic heat exchanger

To cite this article: Carlos Hernando *et al* 2025 *IOP Conf. Ser.: Mater. Sci. Eng.* **1327** 012078

# Thermal characterization of a three-fluid cryogenic heat exchanger

**Carlos Hernando[1,2*], Javier Munilla[2,3], Luis García-Tabarés[3] and Iván Castro[1]**

[1] CYCLOMED TECHNOLOGIES, Madrid, Spain
[2] Comillas Pontifical University, Madrid, Spain
[3] CIEMAT, Madrid, Spain

[*]E-mail: c.hernando@cyclomed.tech

**Abstract.** Magnetic refrigeration, a well-established technique employed to attain temperatures below the Kelvin scale, is currently gaining prominence for its application at temperatures corresponding to liquid helium and liquid hydrogen. This surge in interest is attributable to the elevated Carnot efficiency associated with magnetic refrigeration in such temperature ranges. A test stand has been developed for evaluating heat transfer coefficients of magnetocaloric materials. The system involves a hermetic helium gas circuit cooled to cryogenic temperatures, flowing through a packed bed of magnetocaloric material. A three-fluid heat exchanger is used to cool down the helium gas flowing through the magnetocaloric packed bed. This paper presents the test setup, experimental performance results and the analysis of the three-fluid heat exchanger in the 4.2 K–290 K temperature range. The recorded measurements are juxtaposed against numerical predictions across various mass flow rates and fluid stream pressures. Under nominal operational conditions with helium gas, an outlet temperature of less than 6K is attained, accompanied by a combined pressure drop of merely 2.5 mbar. Furthermore, recommendations for enhancing the design are proposed based on the findings.

## 1. Introduction

Cryocoolers have undergone major advances in the last 20 years, improving their heat rejection capacity, and reliability. However, the cost and Carnot efficiency of these devices are still limiting factors [1] for the development of breakthrough superconducting applications. Magnetic refrigeration is a promising alternative, since the reversible nature of the undergone process delivers high Carnot efficiencies [2]. The magnetocaloric effect (or MCE) [3], is the basis of magnetic refrigeration. For the modelling of a magnetic refrigerator, it is essential to establish the heat transfer and fluid dynamics mechanisms, therefore a test stand is being developed to validate and determine heat transfer coefficients in magnetocaloric regenerators [4].

One of the main components of the setup is a 3-fluid heat exchanger, which is used for recovering the enthalpy of the liquid helium bath where a superconducting magnet is submerged. This recovered enthalpy is transferred to a closed helium gas circuit that flows through the magnetocaloric regenerator and is in charge of cooling it down to cryogenic temperatures. This article presents the design, sizing, and experimental validation of such heat exchanger down to cryogenic temperatures.

## 2. Mathematical modelling and design

*2.1 Heat Exchanger Boundary Conditions*

Figure 1 (left) shows the schematic of the experimental system. It is a closed system that uses a pump to circulate helium through the circuit and inside a cold cryostat. The pressure and mass flow of the system are controlled with four mass flow controllers (MFC), MFC1, MFC2, MFC3 and MFC4. The flow direction inside the cryostat is controlled with three manual valves (MV), allowing the testing of two different materials during the same set of experiments. The helium gas enters a cryostat and is cooled in a 3-fluid heat exchanger (HX), which is a coaxial tubular HX, as depicted in Figure 1 (centre) and schematized in Figure 1 (right). The nomenclature for each fluid is as follows: fluid 1 is the evaporated helium gas from the liquid helium bath, fluid 2 is the helium gas going through the annular area of the heat exchanger, and fluid 3 is the helium gas flowing through the inner tube. Either fluid 2 or fluid 3 could be the high-pressure (HP) fluid.

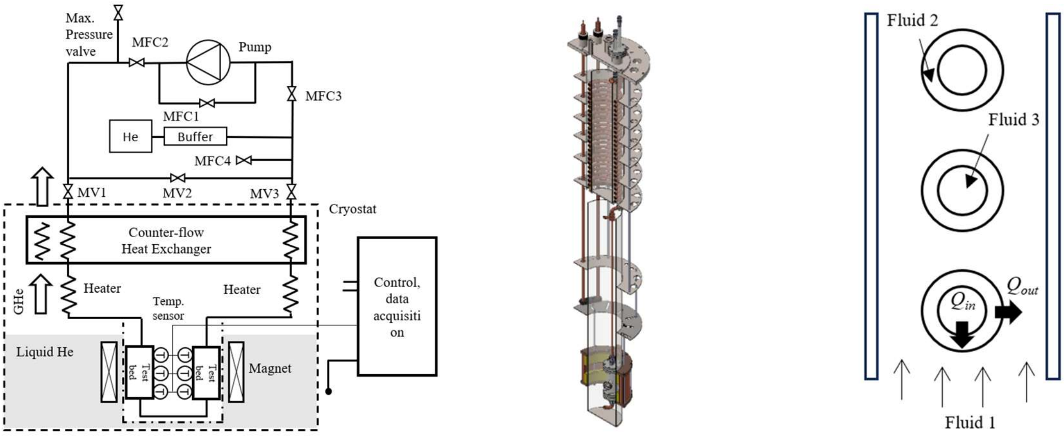


**Figure 1** Schematic of apparatus and data acquisition system (left), the portion enclosed by dashed lines are inside a cryostat. Cryostat side of the test stand (centre). Schematic of the heat exchanger (right)

Figure 2 shows a simplified schematic of the heat exchanger and the boundary conditions for a clockwise flow direction inside the cryostat (fluid 3 as the HP fluid), which is the less effective configuration. The coordinate system of Figure 2 is maintained in all configurations, i.e. point $x = 0$ is always defined at the HP fluid outlet.

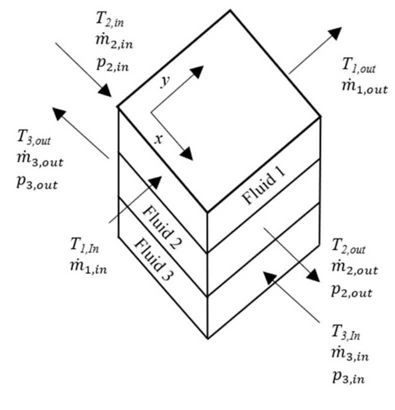


**Figure 2** Boundary conditions of the 3-fluid heat exchanger

**Table 1** BCs and Fluid 3 thermal targets

| Boundary conditions | Values |
|---|---|
| Fluid 1 (Evaporated LHe) | $T_{1,in} = 6\ K$<br>$\dot{m}_{1,in} = 42$ g/min |
| Fluid 2 (LP GHe) | $T_{2,in} = T_{amb}$<br>$T_{2,in} = T_{3,out} + 2\ K$<br>$\dot{m}_{2,in} = \dot{m}_{3,in}$<br>$p_{2,in} = p_{3,out}$ |
| Thermal target | |
| Fluid 3 (HP GHe) | $T_{3,out} = 10K$<br>$\dot{m}_{3,in} = 10\ g/min$<br>$p_{3,in} = 1.5$ bar |

The main objective is to reach a temperature of 10K at the outlet of fluid 3, with a mass flow of 10 g/min. The boundary conditions for fluid 1 are evaluated using information about the cryostat losses and previous tests. The boundary conditions for fluids 2 and 3 are imposed by the rest of the circuit components, mainly the pressure-mass flow curve of the mechanical pump. To increase the safety coefficient of the design, a 2K gradient is added to the inlet fluid 2 temperature with respect to the fluid 3 outlet.

*2.2 Thermohydraulic Modelling*

In the analysis the following list of idealizations and approximations is adopted:

1. The three-fluid heat exchanger operates under steady-state conditions.
2. The heat exchanger is adiabatic; that is, heat losses to the surroundings are negligible.
3. The specific heats and other fluid and material properties are temperature dependent. The properties have been obtained from [5]
4. Non-linear pressure drop, and friction losses have been considered for fluid 2 and 3. No friction losses have been considered for fluid 1.
5. Zero heat conduction is assumed in fluids or in walls parallel to the fluid flow direction.

The dimensionless heat balance equations of the 3-fluid heat exchanger are:

$$\frac{\partial \Theta_1}{\partial \xi} = \mathrm{NTU}_1(\Theta_2 - \Theta_1) \quad (1)$$

$$t\frac{\partial \Theta_2}{\partial \xi} = \mathrm{NTU}_1 C_{12}^*(\Theta_2 - \Theta_1) - \mathrm{NTU}_1 C_{12}^* R^*(\Theta_3 - \Theta_2) - \frac{\mu_{JT,2}}{T_{2,in} - T_{1,in}}\frac{\partial P_2}{\partial \xi} \quad (2)$$

$$-t\frac{\partial \Theta_3}{\partial \xi} = \mathrm{NTU}_1 R^* \frac{C_{12}^*}{C_{23}^*}(\Theta_3 - \Theta_2) - \frac{\mu_{JT,3}}{T_{2,in} - T_{1,in}}\frac{\partial P_3}{\partial \xi} \quad (3)$$

$$t\frac{\partial P_2}{\partial \xi} = f_2\frac{\dot{m}_2^2}{2\rho_2 A_2^2 D_{2,h}}, \qquad -t\frac{\partial P_3}{\partial \xi} = f_3\frac{\dot{m}_3^2}{2\rho_3 A_3^2 D_{3,h}} \quad (4)$$

Where $P_k$ is the pressure of fluid $k$ $(k = 2,3)$, $\mu_{JT,k}$ is the Joule-Thomson coefficient, $f_k$ is the friction factor coefficient, $\rho_k$ is the fluid density, and $A_k$ is the cross section. Variable $t$ indicates the flow direction of the helium circuit, a value of 1 indicates that fluid 2 is the HP fluid, and a value of -1 that fluid 3 is the HP fluid. The nondimensional parameters are defined as follows:

$$\Theta_\mathrm{i} = \frac{T_i - T_{1,in}}{T_{2,in} - T_{1,in}}, \qquad \xi = \frac{x}{X_0} \quad (6)$$

$$NTU1 = \frac{(UA)_{1,2}}{(\dot{m}c_p)_1}, \qquad C_{12}^* = \frac{(\dot{m}c_p)_1}{(\dot{m}c_p)_2}, \qquad C_{23}^* = \frac{(\dot{m}c_p)_3}{(\dot{m}c_p)_2}, \qquad R^* = \frac{(UA)_{3,2}}{(UA)_{1,2}} \quad (7)$$

Where $T_i$ is the temperature of each fluid $(i = 1,2,3)$, $(UA)_{\mathrm{i,j}}$ is the heat transfer coefficient, $U_{i,j}$, multiplied by the heat transfer area, $A_{i,j}$, between two fluids, $(\dot{m}c_p)_\mathrm{i}$ is the heat capacity rate for each fluid, and $X_0$ is the heat exchanger flow length in the x direction. Since the heat exchanger has the form of a spiral, the y direction has been eliminated by a change of variable to reduce the problem dimension: $\partial y = \frac{\partial x * p}{\sqrt{C^2+p^2}}$, where p and C are the pitch and circumference of the heat exchanger. For the computation of the heat transfer and friction factor coefficient the appropriate correlations for each flow regime used in [6] and [7] have been applied.

## 3. Design Analysis

The determination of the dimensions of the heat exchanger is typically categorized as a sizing problem, which is a traditional inverse problem in heat transfer systems. Since there is no explicit closed-form formula for NTU in this case, an iterative approach is used. Due to space, manufacturing limitations, and availability, most of the heat exchanger's parameters were predefined. Only the heat exchanger length was left as the optimization variable.

Figure 3 shows the outlet temperature of fluid 3 as a function of the exchanger's length. It can be observed how the length increases almost exponentially to gain the last tenths of Kelvin. The difficulty in lowering the outlet temperature resides in the imposed boundary conditions, especially the temperature gradient between fluid 2 and fluid 3. Table 2 shows the established dimensions for the heat exchanger, with a final selected length of 10.25 meters.

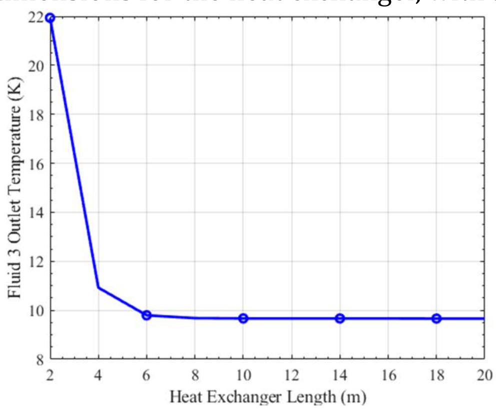


**Table** 2 thermal design values for the 3-fluid HX

| Parameter | Outer Pipe | Inner Pipe |
|---|---|---|
| Pipe Diameter (mm.) | 12 mm. | 6 mm. |
| Pipe Width (mm.) | 1 mm. | 1 mm. |
| $\Delta T$ (K) | 293-12 K | 10-125 K |
| $\Delta p$ (mbar) | 1 mbar | 1.5 mbar |
| Pipe length (m) | 10.25 m | |
| Effectiveness | 98.2% | |
| Pipe Material | Copper | |
| Diameter & Height (mm. x mm.) | 150 mm. x 250 mm. | |

**Figure** 3 Fluid 3 outlet temperature ($\xi = 0$) as function of heat exchanger length

Figure 4 shows the temperature distribution along the heat exchanger for each fluid with the final dimensions. Notably, there is a temperature crossover between fluids 2 and 3 at $\xi = 0.05$, where the heat exchange between the two fluids changes sign.

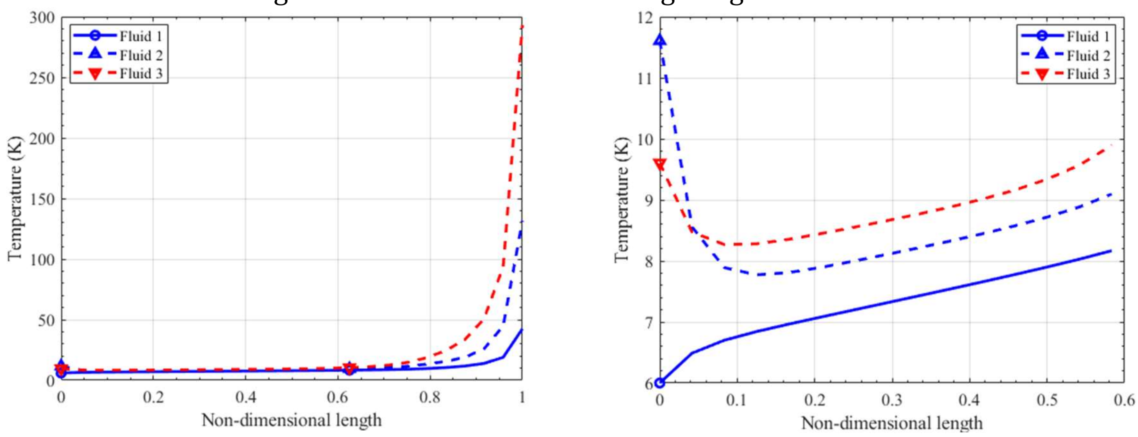


**Figure 4** Temperature evolution along the heat exchanger

Fluid 1's heat is predominantly recuperated at the exchanger's end due to temperature-dependent gas properties affecting the inter-fluid NTU.

Figure 5 (left) shows the evolution of NTU1 across the heat exchanger. The reduction of NTU and the temperature cross at the beginning of the heat exchanger explains the low marginal gain of effectiveness with length shown in Figure 3. Figure 5 (right) shows the pressure loss of each fluid along the heat exchanger. The total pressure loss at nominal conditions is just 2.5mbar.

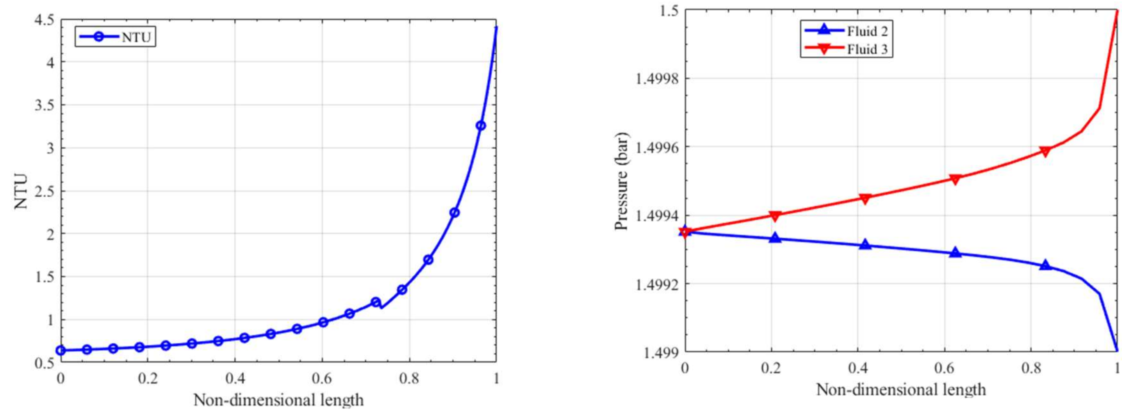


**Figure 5** NTU1, NTU between fluid 1 and fluid 2, evolution along the heat exchanger (left), and pressure evolution along the heat exchanger length

## 4. Experimental Results and Model Correlation

Before the liquid helium tests, the heat exchanger was tested in a liquid nitrogen bath to validate the design and compare the theoretical model against experimental data. The heat exchanger was bypassed at the outlet, connecting the fluid 2 inlet with the fluid 3 outlet, and instrumented with CERNOX temperature sensors at different locations to acquire the real operating data of the 3 fluids. Table 3 shows the measured conditions in each test, which are used as model inputs.

**Table 3.** Measured boundary conditions during heat exchanger characterization

| Test – HP fluid | LN2 Test-Fluid 2 | LN2 Test-Fluid 3 | LHe Test-Fluid 2 | LHe Test-Fluid 3 |
|---|---|---|---|---|
| Fluid 1 (Evaporated cryogen) | $T_{1,in} = 77.8\ K$<br>$\dot{m}_{1,in} = 0.55$ g/s | $T_{1,in} = 77.8\ K$<br>$\dot{m}_{1,in} = 0.55$ g/s | $T_{1,in} = 4.8\ K$<br>$\dot{m}_{1,in} = 0.7$ g/s | $T_{1,in} = 4.8\ K$<br>$\dot{m}_{1,in} = 0.7$ g/s |
| Fluid 2/3 | $T_{2,in} = 290\ K$<br>$T_{3,in} = T_{2,\mathrm{out}}$<br>$p_{2,in} = 1.5\ bar$ | $T_{3,in} = 290\ K$<br>$T_{2,in} = T_{3,out}$<br>$p_{3,in} = 1.5\ bar$ | $T_{2,in} = 288\ K$<br>$T_{3,in} = T_{2,out}$<br>$p_{2,in} = 1.9\ bar$ | $T_{2,in} = 288\ K$<br>$T_{2,in} = T_{3,out}$<br>$p_{3,in} = 1.9\ bar$ |

Figure 6 shows the temperature at the exit of the heat exchanger, against the model expected values. Each test was done in both directions. Figure 6 (left) shows the results using fluid 2 as the high-pressure fluid, and in the right, Figure 6 shows fluid 3 results as the high-pressure fluid.

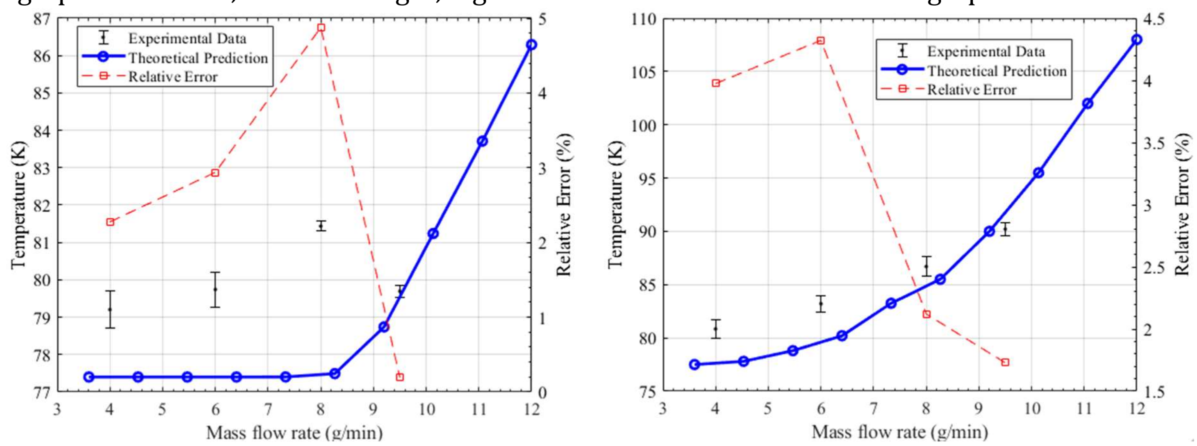


**Figure 6** Fluid 2 (left) and Fluid 3 (right) outlet temperature ($\xi = 0$) as function of fluid 2/3 mass flow during liquid nitrogen testing

Model-data discrepancies likely stem from assumptions, particularly neglecting heat conduction and assuming adiabatic conditions, though results remained sufficiently accurate.

Post-optimization of assembly to reduce losses and boost fluid 1's mass flow enabled final magnetocaloric test stand assembly for LHe testing.

Figure 7 shows the outlet temperatures for the two configurations. Temperature measurements were conducted at the test bed inlet, positioned 450 mm downstream from the heat exchanger outlet. The measured temperatures exhibited slightly lower values than those predicted by the model, likely due to additional heat transfer along the connecting tube between the heat exchanger and test bed. Notably, the primary objective of achieving inlet temperatures below 10K at both test beds was successfully accomplished.

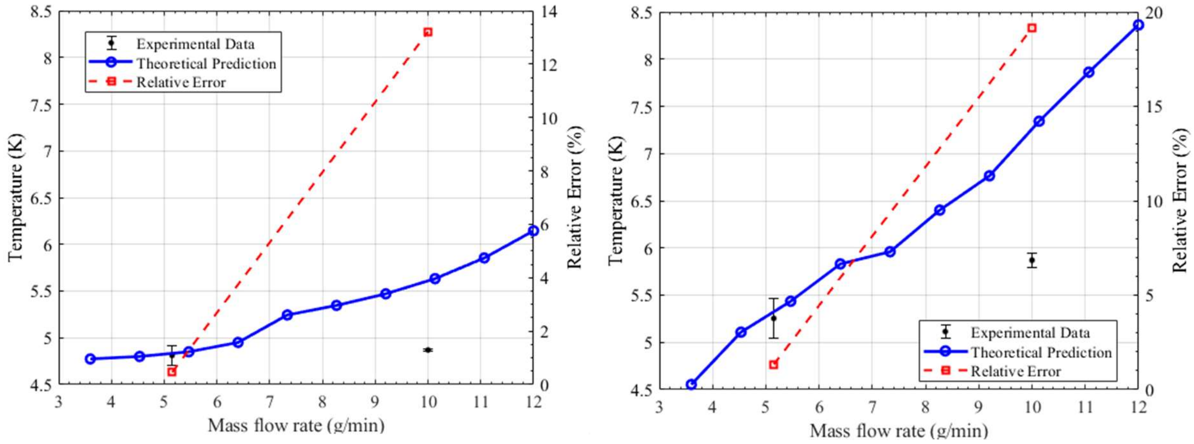


**Figure 7** Fluid 2 (left) and Fluid 3 (right) at the entry of the magnetocaloric regenerator ($\xi = 0$) as function of fluid 2/3 mass flow during liquid helium testing

## 5. Conclusions

A test stand for magnetocaloric materials characterization at cryogenic temperatures is being developed, requiring a three-fluid heat exchanger to cool the helium gas in the closed circuit to 10K. This heat exchanger has been successfully designed, manufactured, and tested, achieving the target temperature, which has enabled the first set of characterization experiments on two magnetocaloric materials: Gadolinium Gallium Garnet ($GGG$) and Erbium Aluminum ($ErAl_2$).

The correlation between the model and experimental data for the heat exchanger was fair, but a more detailed model is needed to accurately predict the heat exchanger's performance. An updated model, which includes conduction and external heat losses, is being developed and validated with additional testing and instrumentation.

## References

[1] R. Radebaugh, “Cryocoolers: the state of the art and recent developments,” *J. Phys. Condens. Matter*, vol. 21, no. 16, p. 164219, 2009, doi: 10.1088/0953-8984/21/16/164219.
[2] V. Franco, J. S. Blázquez, J. J. Ipus, J. Y. Law, L. M. Moreno-Ramírez, and A. Conde, “Magnetocaloric effect: From materials research to refrigeration devices,” *Progress in Materials Science*, vol. 93. Elsevier Ltd, pp. 112–232, Apr. 01, 2018, doi: 10.1016/j.pmatsci.2017.10.005.
[3] E. Brück, “Developments in magnetocaloric refrigeration,” *Journal of Physics D: Applied Physics*, vol. 38, no. 23. IOP Publishing, p. R381, Dec. 07, 2005, doi: 10.1088/0022-3727/38/23/R01.
[4] C. H. Lopez De Toledo *et al.*, “Cryogenic Test Stand for Characterization of Magnetocaloric Materials,” *IEEE Trans. Appl. Supercond.*, vol. 34, no. 3, pp. 1–5, May 2024, doi: 10.1109/TASC.2024.3370126.
[5] “Cryogenics Material Properties.” https://trc.nist.gov/cryogenics/materials/materialproperties.htm (accessed Jan. 18, 2022).
[6] R. F. Barron, *Cryogenic Heat Transfer*, 1st ed. CRC Press, 1999.
[7] W. M. Rohsenow, J. P. Hartnett, and Y. I. Cho, Eds., *Handbook of Heat Transfer*, Third. MCGRAW-HILL, 1997.